A quartz quasimonolith for absolute x-ray wavelength measurements

D. Klöpfel, G. Hölzer, and E. Förster
Max-Planck Arbeitsgruppe ''Röntgenoptik'', an der Friedrich-Schiller-Universität Jena, Max-Wien-Platz 1, D-07743 Jena, Germany

P. Beiersdörfer
Department of Physics and Space Technology, Lawrence Livermore National Laboratory, Livermore, California 94550

(Received 3 February 1997; accepted for publication 28 July 1997)

We have constructed a quasimonolithic crystal consisting of two offset, parallel-mounted quartz $(10\bar{1}0)$ crystals for determining the wavelengths of x-ray transitions on an absolute scale without the need for reference lines. The design and organization of the quasimonolith crystal device, as well as the determination of the relevant parameters and their corresponding uncertainties are discussed. A calibration chain is established that enables linking any wavelength measurement directly to optical wavelength standards and thus to SI units. Our analysis shows that absolute wavelength measurements with an uncertainty of one part per million are in principle possible with the device. Implementation of the quartz quasimonolith in a high-resolution vacuum spectrometer used to study x-ray line emission from an electron beam ion trap is described. © *1997 American Institute of Physics.* [S0034-6748(97)04910-1]

I. INTRODUCTION

Wavelengths of spectral lines in the x-ray region have traditionally been determined by comparison with tabulated reference lines, i.e., it is essential to know the positions of one or more reference lines in the observed spectral range and moreover to know them in SI units to be able to determine the spectral line position also in SI units. In the last decade(s), great efforts have been made in the National Institute of Standards and Technology (USA) and the Physikalisch-Technische Bundesanstalt (Germany) for an absolute calibration of the lattice constants of silicon crystals to optical standards (see, for example, Ref. 1 for a review) as a prerequisite for the determination of the absolute wavelengths of some γ-ray reference lines[2] and a few x-ray reference lines[3,4] by x-ray diffraction. The use of such standards has resulted, for example, in accurate wavelength measurements of x-ray transitions on heavy-ion accelerator facilities[5–7] and tokamaks.[8]

More than 80 years ago, Uhler and Cooksey[9] suggested a method for the measurement of wavelengths, which avoids a comparison with reference lines and allows a direct determination of the wavelengths provided the crystal spacing is otherwise established. This method involved a fixed crystal position and a movable film mounting, the latter of which being shifted by a defined distance between two exposures with a continuous x-ray source. The corresponding shift between the two images of the spectral line on the film plate is characteristic for each wavelength and a determination of the wavelength without using a reference line is possible. Reference lines are, however, often used in the determination of the lattice spacing needed for this approach (see Sec. III D).

The above setup is not appropriate for x-ray flash sources, and a modification was proposed by Förster *et al.*[10] in 1983. The need for two film positions is avoided by the use of a crystal monolith (cf. Fig. 1) consisting of two parallel crystal plates, which create the effect of two offset spectra in a single exposure. No movement of any part of the device is required. As in the original setup described by Uhler and Cooksey, the wavelength can be determined from the separation A of the two images of the spectral line registered on a single detector surface, if the distance between the reflecting crystal plates L and the lattice spacing d of the crystal are known.

A quasimonolithic crystal setup was used experimentally in 1990 to measure wavelengths of laser-produced emission lines.[11] Very high wavelength accuracies were achieved. However, some of the measured wavelengths were found to disagree well outside the cited error limits with subsequent measurements.[12] The disagreement may have been caused by systematic, source-induced errors that were not accounted for, such as line blending, Doppler shifts due to bulk plasma motion, or satellite shifts, which can affect measurements of laser-produced spectra. A clear, well documented analysis of the properties of the quasimonolithic crystal, however, is also needed to understand the possible systematic uncertainties arising from the use of this device. We present such a documentation and characterize the monolith with the highest possible accuracy. Moreover, we describe its implementation on an electron beam ion trap (EBIT). The EBIT source is very well suited for precision x-ray spectroscopy because the source is stationary, spatially narrow, operates in the low-collisional limit, and produces highly charged ions with very low ion temperature.[13,14]

The use of a quasimonolithic crystal enhances the utility of the EBIT source for wavelength measurements by extending the regime over which such measurements can be made. To our knowledge, external x-ray standards have not yet been successfully implemented on the EBIT source, although some attempts are underway.[15] The reason is the difficulty to position the external x-ray source in exactly the same place as EBIT and to ensure that the external source fills the spectrometer optics in precisely the same way as the internally generated radiation from the highly charged ions under investigation. External x-ray standards have, therefore, only

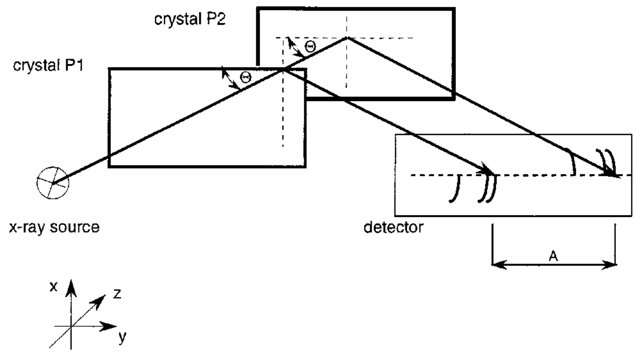

FIG. 1. Basic setup of the quartz quasimonolith.

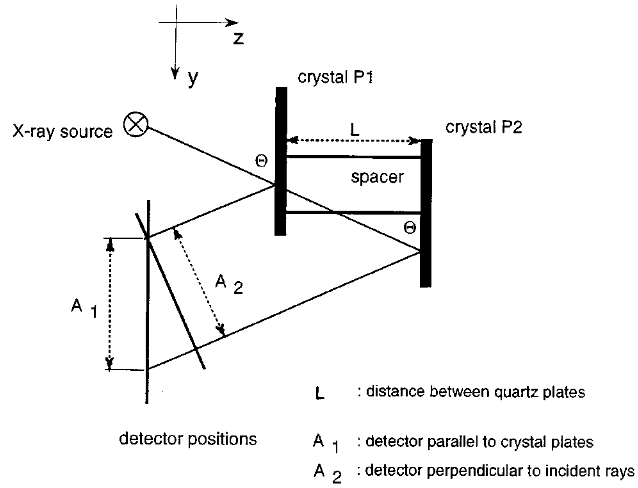

FIG. 2. Schematic of the quasimonolithic setup, showing two possible detector arrangements.

been used to establish the dispersion,[16] but not the absolute wavelength scale. Wavelength measurements performed using the EBIT source so far have relied on internally generated reference lines (e.g., Ref. 12 and 17). For this purpose, internal reference lines from hydrogenic or heliumlike ions have been employed, the wavelength of which was given in most cases by modern atomic structure calculations.[18,19] Uncertainties in the case of the heliumlike reference lines are indicated by comparison of the theoretical reference values with measured values (see, for example, Ref. 20) as well as with new calculations[21] of improved two-electron quantum electrodynamical contributions. These uncertainties limit the accuracy that can be achieved with internal heliumlike reference lines to 10^{-5} or worse. The theoretical values of the hydrogenic reference lines are thought to be known with higher accuracy; but using the calculated values of hydrogenic lines as reference standards precludes the possibility of testing the accuracy of such calculations. The use of a quasimonolithic crystal, in principle, enables measurements with an accuracy near 10^{-6} provided the accuracy of the determination of the lattice spacing is better than this value (which is fulfilled for our measurements, see Sec. III D) and large Bragg angles near 90° are used [see Sec. II, Eqs. (12) and (14)]. This arrangement allows the wavelength measurement of hydrogenic transitions important for testing the accuracy of quantum electrodynamical calculations of one-electron ions. Moreover, wavelength measurements with quasimonolithic crystals are not limited to lines that are close to appropriate hydrogenic or heliumlike reference lines. The proximity to appropriate reference lines is thus no longer a requirement for accurate wavelength determinations.

According to the Bragg equation, a wavelength can be determined with high precision if the Bragg angle can be measured with high precision (neglecting a manyfold of necessary corrections) and the lattice constant of the crystal is known with an equally high precision. By determining the lattice parameter of the spectrometer crystal(s) in SI units (see Sec. III D), a direct calibration of the spectrometer is achieved and a direct and absolute measurement of the wavelength is possible. The accuracy of the wavelength measurements is determined by the precision obtained in determining the monolith parameters L and d. In the following, we demonstrate a measurement of L within 1 μm and of d within 0.5 fm. The accuracy with which these parameters are determined, in principle, allows a wavelength determination with an accuracy of one part per million.

II. ANALYSIS OF THE QUASIMONOLITHIC CRYSTAL SETUP

From the source, x rays of the wavelength λ are incident with a certain angle Θ upon the crystal plates P1 and P2 (cf. Fig. 1) and are reflected when Θ fulfills the corrected form of the Bragg equation:

$$\lambda = 2d\left(\sin\,\Theta - \frac{\delta(\lambda)}{\sin\,\Theta}\right). \tag{1}$$

The correction factor $\delta(\lambda)$ is dependent upon λ and takes into account the deviation of the x-ray refraction index in the crystal from unity. $\delta(\lambda)$ is typically of the order from 10^{-4} to 10^{-3}. The x rays reflected from crystal plates P1 and P2 are then recorded on the detector surface, where the separation of the crystal plates results in a shift A between the two images of a spectral line.

Two detector placements are shown in Fig. 2. The differences arise from the angular position of the detector. In the first, the detector face is placed parallel to the crystal surfaces; in the second, the detector face is oriented perpendicular to the direction of the reflected x rays. The latter setup is needed to avoid line broadening due to parallax effects in a thick detector. The unknown wavelength λ can be evaluated from the shift of the spectrum as follows.

For the detector (film) parallel to P1 and P2, it follows that

$$\cot\,\Theta = \frac{A_1}{2L}. \tag{2}$$

From Eqs. (1) and (2),

$$\lambda = 2d\left(\frac{1}{\sqrt{1+\left(\frac{A_1}{2L}\right)^2}} - \delta(\lambda)\,\sqrt{1+\left(\frac{A_1}{2L}\right)^2}\right). \tag{3}$$

For the detector perpendicular to the incoming x-ray beam, e.g., electronic detector in an $\Theta-2\Theta$ spectrometric setup, it follows that

$$\cos\,\Theta=\frac{A_2}{2L}, \tag{4}$$

where it can be seen that,

$$A_2=A_1\,\sin\,\Theta \tag{5}$$

so that in this case,

$$\lambda=2d\left(\sqrt{1-\left(\frac{A_2}{2L}\right)^2}-\delta(\lambda)\,\frac{1}{\sqrt{1-\left(\frac{A_2}{2L}\right)^2}}\right). \tag{6}$$

The quasimonolithic arrangement is optimized for the wavelengths near the $2d$ value of 0.85 nm. Within this region, which is far from any absorption edge of quartz, a linear approximation of the dependence of the correction factor δ upon wavelength can be found, thereby simplifying the analysis of the measurement

$$\delta(\lambda)=\delta_\lambda\cdot\lambda+\delta_0. \tag{7}$$

Using the reference data from Henke *et al.*[22] for the wavelength dependent atomic scattering factors, we calculated $\delta_\lambda=6\times10^{-4}\ \mathrm{nm}^{-1}$ and $\delta_0=-2.61\times10^{-4}$, where the linearization error $(\Delta\lambda/\lambda)\approx2.2\times10^{-7}$ is negligible in the wavelength range $0.70\leqslant\lambda\leqslant0.85$ nm. After combining Eqs. (6) and (7), λ can be expressed as,

$$\lambda=\frac{1-\left(\frac{A_2}{2L}\right)^2-\delta_0}{\frac{1}{2d}\,\sqrt{1-\left(\frac{A_2}{2L}\right)^2}+\delta_\lambda}. \tag{8}$$

Equation (8) is derived under the assumption that the lattice planes of the crystal plates P1 and P2 are parallel to each other. However, if during the manufacturing of the monolith, the misorientation angle α between the lattice planes in both crystal plates is not equal to zero, Eq. (2) is replaced by

$$\cot(\Theta-\alpha)+\cot(\Theta+\alpha)=\frac{A_1}{L} \tag{9}$$

and Eq. (4) is replaced by

$$\frac{\sin(\Theta+\alpha)}{\cos\,\alpha}\,[\cot(\Theta-\alpha)+\cot(\Theta+\alpha)]=\frac{A_2}{L}. \tag{10}$$

Other possible origins of errors not taken into account in Eqs. (9) and (10) include: slightly different lattice spacings d in the two crystals and small deformations or curvatures of the crystal plates due to the stresses resulting from the mounting of the quartz plates to the spacer. Assuming α is negligible, the error $\Delta\lambda/\lambda$ for a parallel setup [see Eq. (3)] can be expressed as follows:

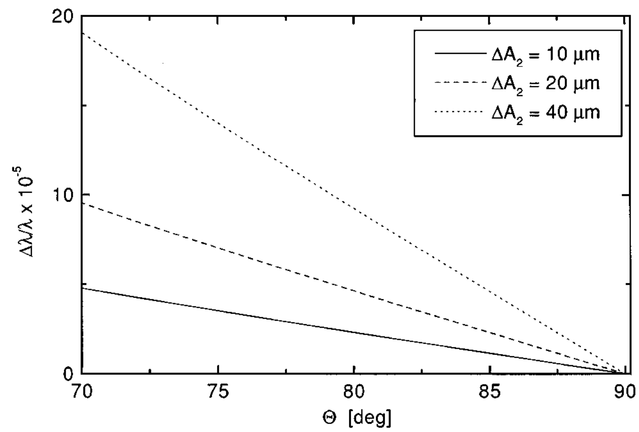

FIG. 3. Calculated resolution $\Delta\lambda/\lambda$ of the quasimonolithic crystal setup as a function of the Bragg angle for different values of the uncertainty ΔA in the determination of the line separation. The detector is assumed to be perpendicular to the incident beam.

$$\left|\frac{\Delta\lambda}{\lambda}\right|=\left|\frac{\Delta d}{d}\right|+\frac{\left(\frac{A_1}{2L}\right)^2}{\left(1+\left(\frac{A_1}{2L}\right)^2\right)}\left[\left|\frac{\Delta A_1}{A_1}\right|+\left|\frac{\Delta L}{L}\right|\right] \tag{11}$$

$$=\left|\frac{\Delta d}{d}\right|+\cos^2\,\Theta\left[\left|\frac{\Delta A_1}{A_1}\right|+\left|\frac{\Delta L}{L}\right|\right] \tag{12}$$

and likewise for a perpendicular-to-incident-beam setup [see Eq. (6)]:

$$\left|\frac{\Delta\lambda}{\lambda}\right|=\left|\frac{\Delta d}{d}\right|+\frac{\left(\frac{A_2}{2L}\right)^2}{\left(1-\left(\frac{A_2}{2L}\right)^2\right)}\left[\left|\frac{\Delta A_2}{A_2}\right|+\left|\frac{\Delta L}{L}\right|\right] \tag{13}$$

$$=\left|\frac{\Delta d}{d}\right|+\cot^2\,\Theta\left[\left|\frac{\Delta A_2}{A_2}\right|+\left|\frac{\Delta L}{L}\right|\right]. \tag{14}$$

Consequently, the accuracy of the wavelength determination is directly proportional to the accuracy of the lattice spacing Δd. The accuracy of the measurement of $A_{1,2}$ and L is weighted by the Bragg angle Θ. The latter dependence was illustrated in Ref.11 for the parallel setup. It is illustrated in Fig. 3 for the setup in which the detector is perpendicular to the incident beam. Here, $\Delta\lambda/\lambda$ is shown for three representative values of ΔA_2 ($\Delta A_2=10$, 20, and 40 μm) for Bragg angles in the range from 70° to 90° and assuming a crystal spacing $L=32.5$ mm corresponding to the spacing in our quasimonolithic crystal. The effect of the error ΔA_2 on the precision of the wavelength determination is rapidly decreasing for $\lambda\rightarrow2d$, i.e., for $\Theta\rightarrow90°$ and large Θ should be used for optimal measurement accuracy. For example, an accuracy of 10 μm in the measurement of A_2 corresponds to a wavelength precision of $\Delta\lambda/\lambda=2\times10^{-5}$ at a Bragg angle of 82.5° and to a precision of 7×10^{-6} at a Bragg angle of 87.5°.

III. EXPERIMENTAL CHARACTERIZATION OF THE QUASIMONOLITH

The main advantage of a quasimonolithic setup over a true monolithic setup is the higher degree of freedom for choosing the geometry of the overall setup. Furthermore, each crystal plate can be independently selected for high crystal perfection and independently prepared and characterized for optimum performance. The main difficulty in setting up a quasimonolithic device arises in establishing a precise connection between the two crystal plates.

The actual setup of the quasimonolith shown schematically in Fig. 2 is as follows. Two quartz plates P1 and P2 (surface orientation $10\bar{1}0$) with the dimensions $40\times 20\times 2.5\ \mathrm{mm}^3$ are mounted onto each side of a quartz glass spacer. The faces of this spacer (length 30 mm, cross section $10\times 15\ \mathrm{mm}^2$) are highly flat and highly parallel (deviation <0.5 arcsec) to each other. The quartz plates are fixed to the spacer by optical contact with a horizontal displacement of 15 mm to allow a larger variation of the angle of incidence. The vertical displacement is 4 mm to allow a simultaneous illumination of both crystal plates (see Fig. 1). Precise determinations of the parameters relevant for accurate wavelength measurements are presented below.

A. Determination of the distance between the quartz plates

In order to measure the distance L between the quartz plates, the three-coordinate measuring machine, UPMC 850 by Carl Zeiss, was employed with an achievable accuracy of 0.1 μm. A survey of the flatness of the crystal surface and the mutual position of both crystal plates is possible using a grid of measurement points on both plates. The x and y axes of the coordinate system measure the height and width of the crystal, while the z axis measures the depth, i.e., the direction between the crystal plates. The reproducibility of the measurements was tested by conducting multiple scans of the object and showed in all directions a maximum deviation of less than 0.2 μm, i.e., the shape of the crystal surfaces can be determined with an accuracy better than 0.4 μm. No deviations of the flatness and the mutual parallelity of the two crystal plates are detectable within this limit.

The average distance L was determined from these measurements to be $(32\,494\pm 1)$ μm. During the measurement, a temperature of 292.8 K was maintained to minimize the influence of the thermal expansion of the quartz glass spacer. The thermal expansion coefficient of quartz glass is $5.1\times 10^{-7}\ \mathrm{K}^{-1}$.[23] Temperature fluctuations smaller than 10 K from the standard temperature, $T_0=293$ K result in an expansion $\Delta L\leqslant 0.2\ \mu$m which may be neglected compared to the accuracy of the measurement ($\pm 1\ \mu$m).

B. Optical interferrometric analysis of the form and parallel positioning of the quartz surfaces

Investigations of the form of the functional surfaces using optical interferrometric methods were made. A Michelson interferrometer was employed to test the parallel mounting of the quartz plates, where a He–Ne laser at $\lambda=0.633\ \mu$m serves as a light source.

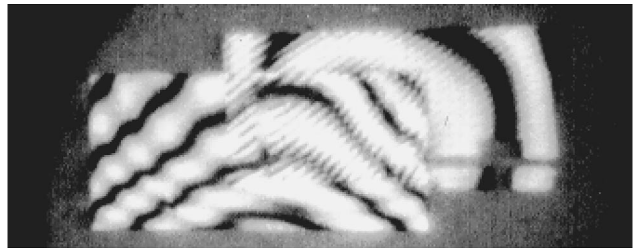

FIG. 4. Interferrometric image showing the precision of the mounting of the two crystal surfaces in relationship to one another.

The interpretation of the interferrograms allows the calculation of the distortion for both crystals in the x and y directions independently. The results reveal that the quartz plates are slightly warped and share a common center of curvature in the vicinity of the glass spacer. The maximum distortion is seen at the corners of the quartz plates, where $\Delta z\leqslant 200$ nm and $\Delta z\leqslant 160$ nm, for the front and back plates, respectively. For x-ray applications, this amount of curvature of the surfaces is negligible. The interferrograms also reveal the tilt of the crystal surfaces to each other (Fig. 4). The tilt in the x (vertical) direction is $10''$; however, more importantly, the tilt in the z (horizontal) direction is very small, $\leqslant 0.5''$.

C. Determination of the misorientation of the lattice planes between the two quartz plates

The validity of Eq. (13) requires that the angle α formed between the lattice planes of both quartz crystals be small, specifically $\alpha\leqslant 10'$ if a measurement accuracy $\Delta\lambda/\lambda\leqslant 5\times 10^{-6}$ is desired in the wavelength range between 0.60 and 0.85 nm. This condition imposes difficulties. To measure an angle with this precision, the measurement of the misorientation of every plate must allow for a maximum uncertainty of $\Delta\alpha\leqslant 5'$. These stringent requirements were met using a combination of optical autocollimator and x-ray diffractometer. The high-performance autocollimation microscope used in the optical adjustment allowed an alignment precision of better than $20''$ of the crystal surface normal. The x-ray diffractometer used a two-circle goniometer as a basis. The quartz quasimonolith was mounted in a special holder that made it possible to measure the absolute tilts for both crystal plates. The reflection $10\bar{1}0$ was studied using Cu $K\alpha_1$ radiation ($\lambda=0.154\,059\,3$ nm, Bragg angle $\Theta_B=10.42°$). The divergence was limited to $\leqslant 2'$ by employing a collimator 350 mm long and a slit with an entrance width of 0.2 mm. For each of the quartz plates, the following test procedure was applied.

First, the surface of the crystal plate was adjusted optically perpendicular to an axis parallel to the surface normal (axis A) with the aid of the autocollimation microscope. Second, the crystal was adjusted for the Bragg reflection with the x-ray diffractometer. The angle of incidence $\omega(\Phi)$ of the x rays for the Bragg reflection was monitored during a full rotation of the crystal around axis A (azimuthal angle Φ), and the maximum $\omega_{\max}$ and minimum $\omega_{\min}$ values were determined. The tilt between the lattice planes and the crystal

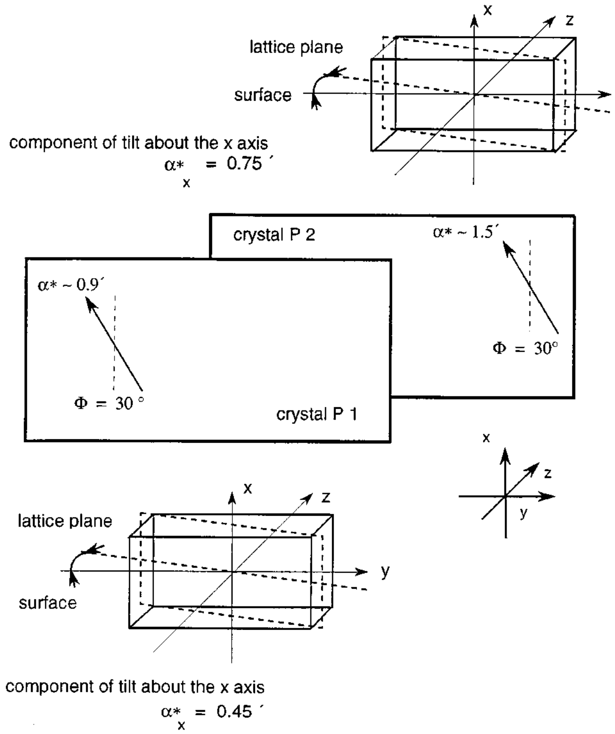

FIG. 5. Schematic showing the misorientation α between the lattice planes of the two crystal plates.

surface for each crystal plate α^* (see Fig. 5) was found from the relationship,

$$\alpha^* = \frac{\omega_{\max} - \omega_{\min}}{2}. \tag{15}$$

The direction of the maximum tilt of the lattice planes to the crystal surface corresponded to the direction of the incident beams (determined by $\Phi_{\max}$ and $\Phi_{\min}$, respectively).

The accuracy for the determination of the extreme values $\omega_{\max}$ and $\omega_{\min}$ was $\leqslant 0.005° (0.3')$, given by the mechanical precision of the goniometer. Taking into account the total possible measurement error involved in the optical adjustment of the crystal surface, the angle between the lattice planes and the crystal surface could be measured with an uncertainty of $\Delta\alpha^* \leqslant 0.6'$.

For both crystal plates, the tilt was greatest for an angle $\Phi_{\max}$ of about 30° to the x axis. The orientation is shown in Fig. 5 in relation to the coordinate system of the quasimonolithic setup. The absolute measured tilt is $\alpha^* \sim 0.9'$ for crystal P1 and $\alpha^* \sim 1.5'$ for crystal P2. Only the x-component α_x^* of α^*, i.e., the component in the diffraction plane, has practical relevance for the precision of the quasimonolith (see Fig. 5). These components amount to $\alpha_x^* \sim 0.45'$ for crystal P1 and $\alpha_x^* \sim 0.75'$ for crystal P2, and correspondingly the tilt between the lattice planes of the crystals P1 and P2 plates relative to another is the difference of these two values, $\alpha_x \sim 0.3'$.

The measured values of the tilts are near the accuracy limits of the instrument. They are much smaller than theoretical value 10′ to achieve the desired resolution of $\Delta\lambda/\lambda \leqslant 5 \times 10^{-6}$ and the lattice plane misorientation can be neglected in the analysis of any wavelength measurements.

TABLE I. Summary of the crystal parameters determined at 293.0 K. Uncertainties reflect 95% confidence limits.

Quantity	Measured value	Uncertainty
L	32 494 μm	± 1 μm
α	$0.3'$	$\pm 20''$
d	0.425 295 6 nm	$\pm 5 \times 10^{-7}$ nm

D. Determination of the lattice plane spacing

As already mentioned in the introduction, the measurement of an absolute wavelength requires that the lattice plane spacing d is measured on the SI scale. The standard method of determining d by x-ray diffraction with x-ray wavelengths as ''length standards'' until recently had limited the achievable accuracy to only a few parts in 10^{-5}, i.e., to the accuracy of the conversion between x-ray units and SI units.[24] Recent measurements using a combination of coupled optical and x-ray interferrometry allowed the determination of the lattice parameter of a silicon crystal in the metric scale with an accuracy of 7×10^{-8}.[25] Such an absolutely calibrated crystal can then be used in turn to determine the wavelength of an x-ray standard, for example, the wavelength of the characteristic radiation from a x-ray tube. This x-ray standard can then be used for a measurement of the lattice spacing d in SI units of any other crystal.

Using this calibration chain, we have determined d of our quartz crystals on an absolute scale. Starting with an absolutely calibrated Si (111) crystal from the Physikalisch–Technische Bundesanstalt (Germany), a determination of the absolute wavelength of the Fe $K\alpha_1$ radiation has been made at the Friedrich–Schiller Universität.[26] The measurement yielded a wavelength of $\lambda = (0.193\,604\,1 \pm 1 \times 10^{-7})$ nm. This enabled us to use the Fe $K\alpha_1$ radiation as a reference standard for determining the lattice spacing d of the quartz quasimonolith. The determination of the lattice spacing of the quartz $(10\bar{1}0)$ planes were performed employing the Bond method[27] and using the high-precision single crystal diffractometer JARD at the Friedrich–Schiller Universität.[28] This instrument is of high mechanical stability; it achieved a mean total angle dividing error of 0.12″ and a minimum step width of 0.06″. The reflection $40\bar{4}0$ (i.e., fourth order of Bragg reflection) was used for the measurement. The results were corrected for instrumental factors and temperature.[29]

The lattice spacing of each quartz plate of the quasimonolith was determined to be $d_{100} = (0.425\,495\,6 \pm 5 \times 10^{-7})$ nm for the standard measuring conditions at 293.15 K. This value represents the mean of 20 independent measurements on each crystal plate. The thermal expansion coefficient of quartz is 1.37×10^{-5} K^{-1} for any direction perpendicular to the crystallographic c axis.[30] The value of d thus changes significantly (in relation to the desired precision of our wavelength measurement) for temperatures that differ by 1 K or more from the standard temperature, and appropriate corrections must be taken into account.

E. Summary of the measurements

A summary of the measured parameters of the quartz quasimonolith is given in Table I. According to Eqs. (12)

and (14), the accuracy of d allows a wavelength determination within one part per million or 1×10^{-6}. By contrast, the relative accuracy of L is only 3×10^{-5}. Because the uncertainty in L is multiplied by a $\cos^2\Theta$ or $\cot^2\Theta$ term, this does not limit the accuracy of a wavelength determination provided the Bragg angle of the measurement is 80° or larger. For $\Theta\geqslant80°$, the weighted uncertainty is less than 1×10^{-6}, i.e., less than the uncertainty of d. Finally, the value of α is sufficiently small to add a negligible amount to the measurement uncertainty.

IV. IMPLEMENTATION ON AN ELECTRON BEAM ION TRAP

A crystal quasimonolith is well suited for implementation on an EBIT device. The reason is that the electron beam configuration of an EBIT represents a line source with a width close to what one would choose for the entrance slit of a flat-crystal spectrometer.[31] The x-ray emitting region in an EBIT is determined by the 60 μm width of the electron beam and the 2 cm length of the trap. A separate entrance slit is therefore not necessary.

A slitless configuration was successfully used in several high-resolution crystal spectrometers on the Livermore EBIT,[31–33] including a very high-resolution flat-crystal spectrometer for the soft x-ray region.[34] To test the performance of the quartz quasimonolith on an EBIT source, it was employed in the latter spectrometer. Designed for measuring low-energy x rays at large Bragg angles, this spectrometer operated *in vacuo* and used a position-sensitive gas proportional counter with a 4-μm-thin polypropylene window for recording.[34] The face of the detector was arranged perpendicular to the incoming x rays, corresponding to detector position 2 in Fig. 2. This geometry avoided line broadening caused by parallax in the 1-cm-deep detector.

Because the quasimonolith performs best for large Bragg angles, i.e., for x-ray lines with wavelength close to twice the lattice spacing of the crystal, we chose to look at the $(2s_{1/2}\,2p^6\,3p_{1/2})_{J=1}\rightarrow(2s^2\,2p^6)_{J=0}$ transition in neonlike Ge^{22+}. This transition had been measured before on EBIT relative to other x-ray lines yielding in a wavelength of about 0.842 13 nm.[12] This wavelength was close to our measured value of $2d=0.850\,591\,2(10)$ nm for the quartz plates of the quasimonolith. The corresponding Bragg angle of our measurement was thus close to 82°.

Germanium was injected into EBIT and sequentially ionized to the neonlike charge state in the interaction with a 65 mA, 2.0 keV electron beam. The energy is well above the 880 eV required to ionize sodiumlike Ge^{21+}, and well below the 2179 eV required to ionize neonlike Ge^{22+}. The resulting charge balance achieved in EBIT is thus overwhelmingly dominated by neonlike Ge^{22+}.

The spectrum of the $(2s_{1/2}\,2p^6\,3p_{1/2})_{J=1}\rightarrow(2s^2\,2p^6)_{J=0}$ transition in Ge^{22+} obtained during a 5 1/2 h period is shown in Fig. 6. The two images of the Ge^{22+} line shifted in relation to one another due to the diffraction at the two crystal plates of the monolith are clearly seen in the figure.

In accordance with Eq. (8), the wavelength of the line depends on the displacement of the two images. The displacement was determined by fitting each image with a Voigt profile. The Voigt profile fit is shown in Fig. 6. The fit procedure used the weighted least squares method. The fit considerably aided in a precise determination of the peak position. This is especially important because the count rate on an EBIT source is generally small. We were able to determine the centerposition of each line to within 100 μm. This corresponds to about 7% of the spatial full width at half-maximum of each line on the detector, resulting in $\Delta A_2/A_2\approx0.01$. The error involved with the evaluation of the distances between the peaks thus typically contributes the most to the overall uncertainty.

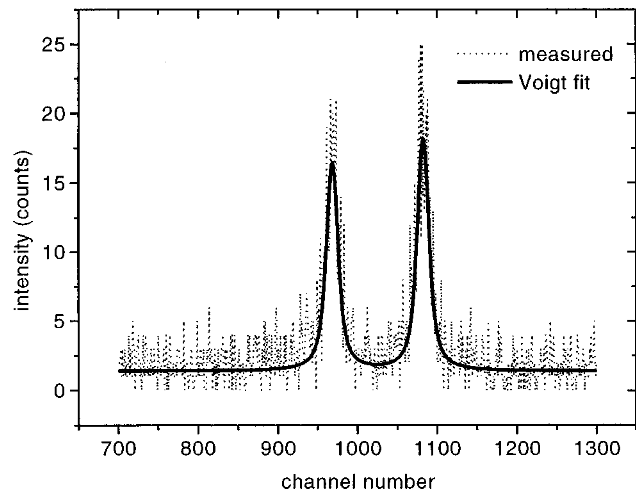

FIG. 6. Spectrum of the $(2s_{1/2}\,2p^6\,3p_{1/2})_{J=1}\rightarrow(2s^2\,2p^6)_{J=0}$ transition in neonlike Ge^{22+} measured with the quartz quasimonolith and best fit using Voigt profiles. The position sensitive detector was calibrated in a separate measurement using a movable slit. One channel corresponds to 0.081 mm.

Having determined the separation of the two images, the wavelength of the $(2s_{1/2}\,2p^6\,3p_{1/2})_{J=1}\rightarrow(2s^2\,2p^6)_{J=0}$ transition in neonlike Ge^{22+} was calculated according to Eq. (8). Two important corrections must be considered:

(1) The calculation was done iteratively in order to correct exactly for the refraction, which is wavelength dependent. Disregarding the refraction correction generally would result in a value that is systematically too small. The difference is about -2×10^{-4} nm in this case.
(2) The value of d must be adjusted to reflect the value appropriate for the temperature of the measurement. The temperature of the crystal was determined to be 298.2 K and was monitored with an accuracy of 0.1 K. By contrast, the value of d is valid for a temperature of 293.15 K (standard measurement conditions). The value of d appropriate for the conditions of the measurement was determined from the temperature expansion coefficient of quartz, which equals 1.37×10^{-5} K^{-1} for any direction perpendicular to the crystallographic c axis.[30]

From the data in Fig. 6 we determine a wavelength of 0.8422 nm for the Ge line. The uncertainty of the measurement is ±0.0002 nm with a 68% confidence limit, or a relative accuracy of 3×10^{-4}. This is much less than the accuracy achievable based on the accuracy of the crystal parameters listed in Table I. The present uncertainty is completely dominated by the uncertainty with which the separation of the two images could be determined, which in this particular example is mainly determined by the low counting statistics, i.e., the low counting rate. Although less accurate, the measured value compares favorably to the value of 0.8423 ± 0.0003 nm reported by Boiko *et al.*[35] and to the value of 0.8427 ± 0.0005 nm reported by Gordon *et al.*,[36] as well as to the newer result of $0.842\,13 \pm 0.000\,06$ nm reported by Nilsen *et al.*[12] with a 68% confidence limit.

The accuracy of the wavelength measurement can be improved, if the separation of the two image lines is measured with higher accuracy. In principle, this can be done by either increasing the number of photons detected, i.e., by improving the counting statistics, or by narrowing the width of the observed lines. The width of the Ge line observed with the quasimonolith is 1.65×10^{-4} nm, or $\Delta\lambda/\lambda = 1.96 \times 10^{-4}$. This value is much larger than that given by the spatial resolving power of the gas proportional counter used in the spectrometer. Instead, it is comparable to the value of ion temperature expected under these operating conditions.[13] If the width arose solely from the thermal motion of the ions in EBIT, it would correspond to an ion temperature of 496 eV. A reduction in the ion temperature could thus bring an improvement in the observed linewidth. Such an improvement, however, cannot go beyond the intrinsic resolving power of the $(10\bar{1}0)$ cut of quartz, which is $\Delta\lambda/\lambda \approx 1 \times 10^{-4}$ and only a factor of 2 better than the observed width. It is, therefore, not possible to drastically improve the accuracy of the wavelength measurement by narrowing the width of the observed lines. A significantly higher wavelength accuracy, i.e., by a factor of 10 or more can be achieved only by measuring brighter x-ray lines or by much longer exposures to record more photons.

Further wavelength measurements with the present quartz quasimonolith are in progress and will be published elsewhere.

ACKNOWLEDGMENT

This work was performed in part by Lawrence Livermore National Laboratory under the auspices of the U. S. Department of Energy under Contract No. W-7405-ENG-48. We thank P. Becker (Physikalisch–Technische Bundesanstalt Braunschweig, Germany) for the providing us with a calibrated silicon crystal for the measurement of the lattice plane distance and O. Wehrhan for the valuable help during the characterization of the quartz quasimonolith.

[1] R. D. Deslattes, in *The Art of Measurement*, edited by B. Kramer (VCH, Verlagsgesellschaft, 1988), p. 193.
[2] R. D. Deslattes, E. G. Kessler, W. C. Sauder, and A. Henins, Ann. Phys. **129**, 378 (1980).
[3] J. Härtwig, S. Grosswig, P. Becker, and D. Windisch, Phys. Status Solidi A **125**, 79 (1991).
[4] G. Hölzer, M. Fritsch, M. Deutsch, J. Härtwig, and E. Förster, Phys. Rev. A (in press).
[5] J. P. Briand, M. Tavernier, P. Indelicato, R. Marrus, and H. Gould, Phys. Rev. Lett. **50**, 832 (1983).
[6] H. F. Beyer, R. D. Deslattes, F. Folkmann, and R. E. LaVilla, J. Phys. B **18**, 207 (1985).
[7] H. F. Beyer, P. Indelicato, K. D. Finlayson, D. Liesen, and R. D. Deslattes, Phys. Rev. A **43**, 223 (1991).
[8] E. S. Marmar, J. E. Rice, E. Källne, J. Källne, and R. E. LaVilla, Phys. Rev. A **33**, 774 (1986).
[9] H. S. Uhler and C. D. Cooksey, Phys. Rev. **10**, 645 (1917).
[10] E. Förster, K. Goetz, S. Grosswig, K. Schäfer, W. D. Zimmer, and K. Sander, Preprint FSU Jena N/83/38, 1983 (unpublished).
[11] A. V. Rodé, A. M. Maksimchuk, G. V. Sklizkov, A. Ridgeley, C. Danson, N. Rizvi, R. Bann, E. Förster, K. Goetz, and I. Uschmann, J. X-Ray Sci. Technol. **2**, 149 (1990).
[12] J. Nilsen, P. Beiersdorfer, S. R. Elliott, T. W. Phillips, B. A. Bryunetkin, V. M. Dyakin, T. A. Pikuz, A. Ya. Faenov, S. A. Pikuz, S. von Goeler, M. Bitter, P. A. Loboda, V. A. Lykov, and V. Yu. Politov, Phys. Rev. A **50**, 2143 (1994).
[13] P. Beiersdorfer, V. Decaux, S. R. Elliott, K. Widman, and K. Wong, Rev. Sci. Instrum. **66**, 303 (1995).
[14] P. Beiersdorfer, V. Decaux, A. L. Osterheld, and K. Widman, Phys. Rev. Lett. **77**, 5353 (1996).
[15] J. D. Gillaspy, Y. Aglitskiy, E. W. Bell, C. M. Brown, C. T. Chantler, R. D. Deslattes, U. Feldman, L. T. Hudson, J. M. Laming, E. S. Meyer, J. Morgan, C. A. Pikin, A. I. Roberts, J. R. Ratliff, L. P. Serpa, F. G. Sugar, and E. Takács, Phys. Scr. **T59**, 392 (1995).
[16] T. E. Cowan, C. Bennett, D. Dietrich, J. V. Bixler, C. J. Hailey, J. R. Henderson, D. A. Knapp, M. A. Levine, R. E. Marrs, and M. B. Schneider, Phys. Rev. Lett. **66**, 1150 (1991).
[17] P. Beiersdorfer, A. Osterheld, S. R. Elliott, M. H. Chen, D. Knapp, and K. Reed, Phys. Rev. A **52**, 2693 (1995).
[18] W. R. Johnson and G. Soff, At. Data Nucl. Data Tables **33**, 405 (1985).
[19] G. W. F. Drake, Can. J. Phys. **66**, 586 (1988).
[20] P. Beiersdorfer, M. Bitter, S. von Goeler, and K. W. Hill, Phys. Rev. A **40**, 150 (1989).
[21] K. T. Cheng, M. H. Chen, W. R. Johnson, and J. Sapirstein, Phys. Rev. A **50**, 247 (1994).
[22] B. L. Henke, E. M. Gullikson, and J. C. Davis, At. Data Nucl. Data Tables **54**, 181 (1993).
[23] Physical Data for Quartz, Jena GmbH Quarzschmelze, Göschwitzer Str. 20, 07745 Jena-Burgau, Germany (unpublished).
[24] J. Bearden, Rev. Mod. Phys. **39**, 78 (1967).
[25] D. Windisch and P. Becker, Phys. Status Solidi A **118**, 379 (1990).
[26] M. Fritsch, Ph.D. thesis FSU Jena, 1996.
[27] W. Bond, Acta Crystallogr. **13**, 814 (1960).
[28] S. Grosswig, J. Härtwig, H.-J. Jäckel, R. Kittner, and W. Melle, Sci. Instrument. **1**, 29 (1986).
[29] J. Härtwig and S. Grosswig, Phys. Status Solidi A **115**, 369 (1989).
[30] J. C. Brice, Rev. Mod. Phys. **57**, 105 (1985).
[31] P. Beiersdorfer, R. E. Marrs, J. R. Henderson, D. A. Knapp, M. A. Levine, D. B. Platt, M. B. Schneider, D. A. Vogel, and K. L. Wong, Rev. Sci. Instrum. **61**, 2338 (1990).
[32] P. Beiersdorfer and B. J. Wargelin, Rev. Sci. Instrum. **65**, 13 (1994).
[33] K. Widman, P. Beiersdorfer, G. V. Brown, J. R. Crespo López-Urrutia, V. Decaux, and D. W. Savin, Rev. Sci. Instrum. **68**, 1087 (1997).
[34] P. Beiersdorfer, J. R. Crespo López-Urrutia, E. Förster, J. Mahiri, and K. Widman, Rev. Sci. Instrum. **68**, 1077 (1997).
[35] V. A. Boiko, A. Y. Faenov, and S. A. Pikuz, J. Quant. Spectrosc. Radiat. Transf. **19**, 11 (1978).
[36] H. Gordon, M. G. Hobby, N. J. Peacock, and R. D. Cowan, J. Phys. B **12**, 881 (1979).